Desalination and Water Treatment
www.deswater.com

doi: 10.5004/dwt.2021.27644

240 (2021) 124–136
November

Pre-treated Moroccan natural clays: application to the wastewater treatment of textile industry

Hayat Loukili[a,b,*], Jamal Mabrouki[c], Abdelkader Anouzla[b], Youness Kouzi[a], Saad Alami Younssi[a], Khalid Digua[b], Younes Abrouki[c]

[a]*Laboratory of Materials, Membranes and Environment, Faculty of Science and Technology Mohammedia, Hassan II University of Casablanca, Morocco, emails: hayat.loukili@fstm.ac.ma (H. Loukili), eespaciodeco@gmail.com (Y. Kouzi), smmdalami@gmail.com (S. Alami Younssi)*
[b]*Laboratory of Process Engineering and Environment, Faculty of Science and Technology Mohammedia, Hassan II University of Casablanca, Morocco, emails: aanouzla@gmail.com (A. Anouzla), khalid.digua@fstm.ac.ma (K. Digua)*
[c]*Laboratory of Spectroscopy, Molecular Modeling, Materials, Nanomaterial, Water and Environment, Faculty of Science, Mohammed V University in Rabat, Rabat, Morocco, emails: jamal.mabrouki@um5r.ac.ma (J. Mabrouki), y.abrouki@um5r.ac.ma (Y. Abrouki)*

Received 29 May 2021; Accepted 20 July 2021

ABSTRACT

The current study was carried out to examine the pre-treated Moroccan natural clays for the removal of methylene blue dye by the adsorption method. The adsorbent was characterized by X-ray diffraction, Fourier transform infrared spectroscopy, scanning electron microscopy. After performing the experiment and analyzing the data, it was found that the optimum conditions for fixing yellow marl and kaolinite (0.05 mm) are 93%–98%. The adsorption kinetics of methylene blue on kaolinite (C = 300 ppm, 50 μm) and on yellow marl (C = 500 ppm, 50 μm) is very efficient. Kaolinite adsorbed better towards basic pH. The equilibrium adsorbed amounts reached 27.5 mg g^{-1} for yellow marl and 16 mg g^{-1} for kaolinite. Application of the membranes developed in the treatment of dyes shows that the rejection rates obtained depend on the charge of the ions, their sizes, the charge of the membrane linked to the pH of the filtered solution. The difference in adsorption capacity between the two clays studied is due to the percentage of the clay phase in each and its composition.

Keywords: Moroccan natural clays; Wastewater treatment; Textile dye; Adsorption

1. Introduction

The quality and availability of water resources are undoubtedly one of the major challenges of our century. Its preservation requires better management of pollutants, mainly from human activities [1]. Let us see where water resource pollution comes from and what measures exist to control it and reduce the threat it poses to our environment. Water pollution is characterised by the presence of micro-organisms, chemical substances or industrial waste. It can affect rivers, groundwater, brackish water, but also rainwater [2]. In addition to the toxicity caused by chemical agents to exposed organisms, genotypic and mutagenic effects have been found to be of concern, causing several health problems and also affecting future generations due to hereditary alterations of genetic material [3–6].

The discharge of industrial effluents is strictly controlled and regulated and in order to control and estimate

---

* Corresponding author.

Presented at the Second International Symposium on Nanomaterials and Membrane Science for Water, Energy and Environment (SNMS-2021), June 1–2, 2022, Tangier, Morocco

the evolution of the main industrial discharges, the laws and regulations have defined the modalities for monitoring these discharges. Self-monitoring is therefore imposed on the largest polluters, considering that these industrialists are responsible for controlling the quality of their discharges [7]. A prefectural decree prescribes the nature and frequency of the measurements to be carried out by the operator himself while following the standards for sampling and analysis of the samples [8].

Chemical oxidation techniques are generally applied in the literature for the treatment of organic hazardous compounds present in low concentrations, as a pre-treatment before biological processes, the treatment of wastewater loaded with constituents resistant to biodegradation methods and as a post-treatment to minimise aquatic toxicity. In general, wastewater treatment in the textile industry is based on physical-chemical and biological treatment [8–11]. During adsorption, the pollutant is removed from the liquid phase to the solid phase. Activated carbon is the most widely used adsorbent for colour reduction, but it is very costly and requires regeneration [12]. It is in this context that we are interested in the valorisation of a food industry reject, which is olive pumice, to use as an adsorbent for the decolourisation of textile industry rejects. Other research has chosen to develop or use other less expensive natural materials (sawdust, wood bark and flour, etc.) for the extraction of dyes by means of adsorption [13,14]. Despite its efficiency, activated carbon remains an expensive and mostly imported material, and the search for new products from a cheap and available source is proving useful. We were interested in the adsorbent properties of clays that could be used in the treatment of waste from the textile industry [15,16]. The use of clay in a new treatment process would be in line with sustainable development, both from an ecological and a societal point of view; but it is also necessary to take into account the economic aspect and therefore to try to use a local clay close to the industry in order to reduce transport costs. The objective of our work, we have characterized the two clays studied by studying their adsorption capacity of methylene blue and heavy metals. The application is to develop a model of treatment of textile wastewater using local products, such as the valorisation of Moroccan natural clays (yellow marl and kaolinite) in the treatment of water from the textile industry.

2. Materials and methods

2.1. Materials and apparatus

All of the reagents were of analytical grade with the mass fraction purity of 0.99 and used as received without further purification. Methylene blue (MB) was purchased from Sigma-Aldrich Company (USA) and was used as received. The MB dye stock solution was prepared by accurately dissolving a weight of dye in distilled water to the concentration of 1 g L^{-1}. The experimental solutions were obtained by diluting the dye stock solution in accurate proportions to needed inlet concentrations.

The adsorbents used in this study are Moroccan clays, namely yellow marl and kaolinite. The arrangement of clay particles is studied via scanning electron microscopy (SEM) using scanning electron microscope Hitachi S-4500 (Japan), the degree of hydration of clay assemblages is obtained via thermogravimetric analysis (TGA) and differential thermal analysis (DTA) using SDT 2960 simultaneous DSC-TGA instruments. The molecular-scale study is achieved by infrared (IR) spectroscopy using Nicolet ZDX FTIR spectrometer (USA). The mineralogical composition of clay assemblages is deduced from X-ray diffraction spectra using X'Pert Pro MRD. Semi-quantitative analysis was performed by energy-dispersive X-ray spectroscopy (EDX) coupled to the LEICA S-260 scanning electron microscope (Germany). The granulometric analysis of the clay powder is carried out using AccuSizer Optical Particle Sizer Model 770.

2.2. Preparation of adsorbents

The yellow marl and kaolinite were pre-treated by acid attack according to the following protocol: a mixture of 1 g of clay and 50 mL of nitric acid (0.1 M) was stirred for 24 h. Centrifugation of this mixture allows the solid phase to be collected and washed with water to eliminate the excess of H^+ ions. The clay obtained after washing with distilled water and drying in an oven at 100°C for 24 h will be kept for later use.

2.3. Sorption capacity and removal efficiency

This part represents the contribution to the study of the surface properties of yellow marl and kaolinite during the adsorption of methylene blue. This dye is used to study the adsorption capacity of solids and to determine their specific surface area and has been the subject of several works [15,17–19]. The choice of this dye lies in the fact that it behaves like a positively charged organic molecule in solution. The adsorption of methylene blue is carried out in a batch reactor. Masses (m) of adsorbent of 1 g are introduced, to which the same volume (50 mL) of methylene blue solution of different concentrations is added. These closed bottles are placed on a stirring table for an average contact time of 4 h at room temperature, after which equilibrium between the different phases is supposed to be reached. The contents of the flask were then centrifuged and the filtrates were analysed by a spectrophotometer (UNICAM UV/Vis Spectrometer) at a wavelength of 664 nm. The pH of the solutions was measured before and after adsorption. The determination of the adsorption kinetics of the two clays and the influence of the physico-chemical parameters (pH, solute concentration and granulometry) are studied. The removal efficiency (Re) is calculated by Eq. (1):

$$\text{Re} = 100 \times \frac{C_0 - C_e}{C_e} \qquad (1)$$

where C_0 is the initial concentration of methylene blue (mg L^{-1}) and C_e is the final concentration of methylene blue after adsorption (mg L^{-1}).

The quantities of methylene blue fixed on the clay is calculated by the sorption capacity (q_e) according to the following equation:

$$q_e = V \times \frac{C_0 - C_e}{m} \qquad (2)$$

where q_e is the uptake capacity (mg g^{-1}), C_0 and C_e (mg L^{-1}) are the liquid-phase concentrations of MB at initial and any time t, respectively, V is the volume of the solution (mL) and m is the mass of the adsorbent (g).

3. Results and discussion

3.1. Characterization of clays

3.1.1. Yellow marl

The yellow marl used comes from the Rabat-Salé region. The samples taken are air-dried for a week, then crushed to obtain small grains and sieved to get rid of larger particles. The yellow marl clay powder is ground to a particle size of £125 µm after crushing and sieving.

Fig. 1 shows the particle size distribution of the powder using a particle size analyzer. It can be seen that there is a significant proportion of particles smaller than 5 µm.

The morphology of the powders was observed using SEM. Fig. 2 shows the morphology of a sample of raw yellow marl sieved to 125 and 50 µm, it shows that the powders are formed of agglomerates of small particles and also indicates the presence of laminated grains in the structure.

The EDX analysis of the raw yellow marl and the fraction below 125 µm are shown in Figs. 3 and 4. From these figures, it can be seen that the two spectra indicate the presence of silica, aluminum, magnesium and calcium. The mass and atomic percentages of these elements are given in Table 1. The change from raw marl to the fraction below 125 µm shows the decrease in the percentage of calcium and the increase in the percentage of silica and aluminum.

An X-ray diffraction pattern was performed on the raw and calcined powder at different temperatures of 600°C and 1,150°C as shown in Fig. 5.

The diffraction patterns of the raw samples reveal the presence of silica mainly in the form of quartz, carbonate and dolomite. Heat treatment at 600°C and 1,150°C is accompanied by a decrease in the calcite line, an increase in the dolomite line and the appearance at 1,150°C of a new mullite phase resulting from the formation of a calcium silico-aluminate.

Thermal analysis TGA/DTA for yellow marl treated at various temperatures are shown in Figs. 6–8.

From Fig. 6, the TGA curve of the yellow marl (fraction < 0.125 mm) recorded during heating indicated a total loss of 22% of the initial sample mass. This loss of weight occurs in two distinct stages, the first at 250°C corresponds to that of the absorbed water and the second at around 650°C corresponds to the departure of the constitutive water to which is added the release of CO_2. Above 800°C the loss of mass remains negligible. On the DTA curve, four endothermic peaks are observed at 68.0°C, 250.63°C, 572°C and 756.71°C, which corresponds respectively to the departure of wet water, to the departure of water adsorbed in the inter-pillar space, to the presence of quartz and to the decomposition of $CaCO_3$. To this is added the presence of an exothermic peak at around 894.64°C which corresponds to the formation of a calcium silico-aluminate.

The TGA/DTA curves of the yellow marl treated at 600°C and 1,150°C respectively, as shown in Figs. 7 and 8. For the TGA, a total mass loss of 17.43% for the marl treated at 600°C and no loss for the marl treated at 1,150°C. This is explained by the fact that at 600°C there is still some organic matter present in the sample. For the DTA, at 600°C we have the same reactions as for the raw clay, beyond 1,150°C no weight loss is observed.

Infrared spectroscopic analysis of yellow marl treated at various temperatures is shown in Fig. 9.

According to Fig. 9, we see the presence of ten main absorption bands for raw yellow marl namely at 3,650 and 3,620 cm^{-1} due to vibrations of hydroxyl groups, at 3,420 cm^{-1} due to hydroxyl groups in water, at 945 and 915 cm^{-1} due to deformation vibrations of the Al–OH bond, at 1,400 cm^{-1} attributed to the presence of carbonate, at 800 and 796 cm^{-1}

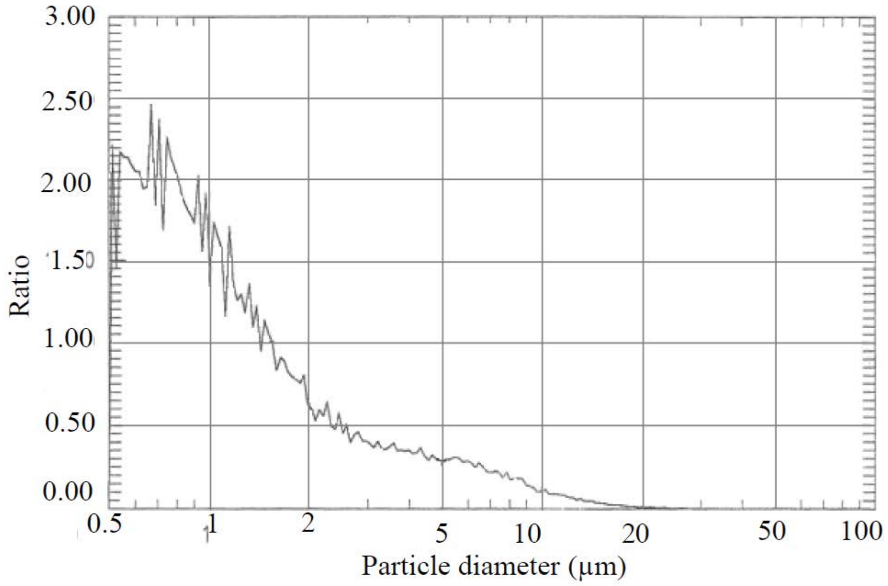

Fig. 1. Size distribution of the powder yellow marl sieved to <125 µm.

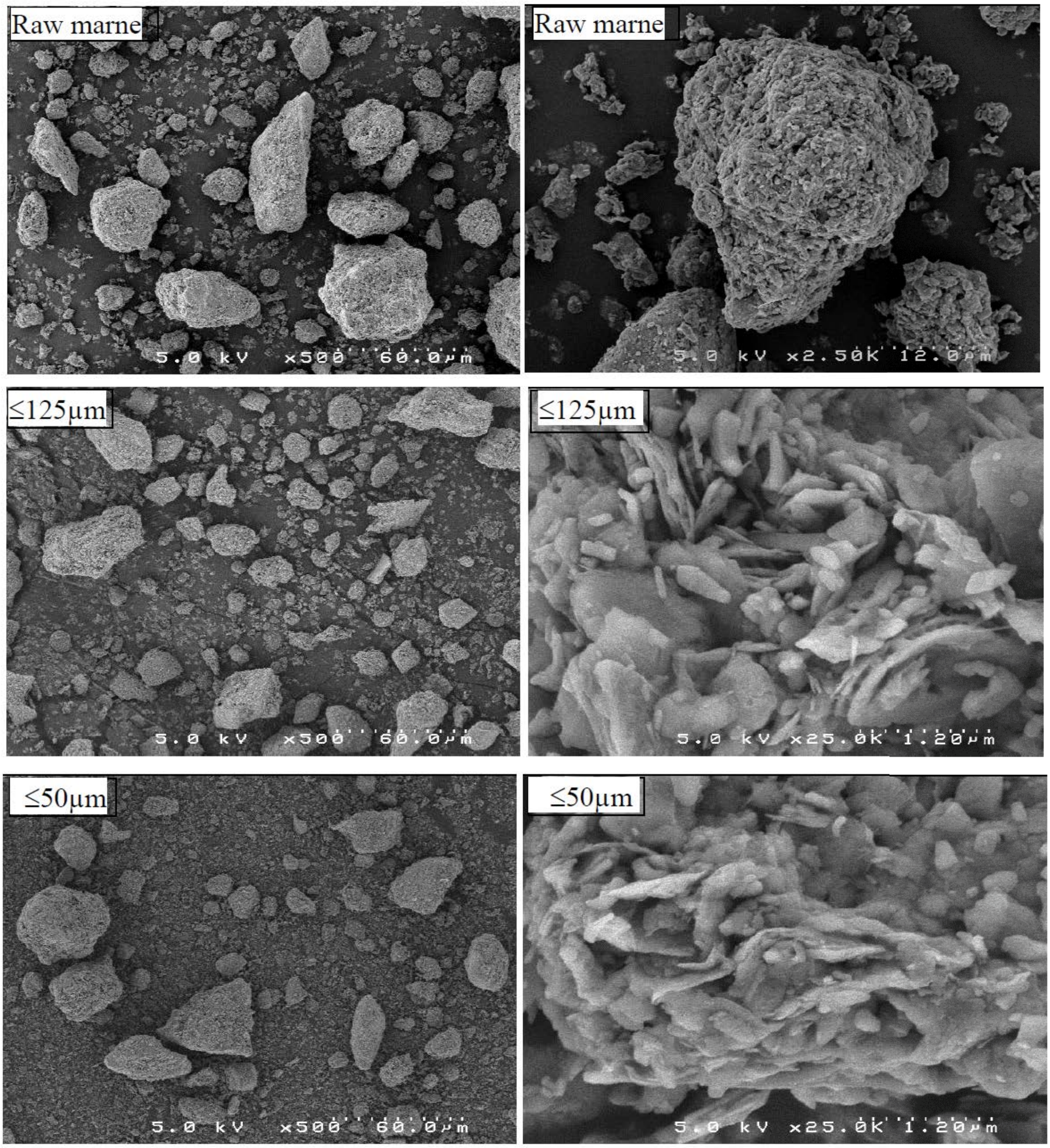

Fig. 2. SEM of the raw yellow marl and the fractions below 125 and 50 μm.

reflecting the symmetrical valence band of quartz and at 530 and 400 cm^{-1} due to the Si–O bond deformation of quartz. In this figure, it can also be seen that the calcining of the sample at 1,150°C resulted in the disappearance of the phyllite bands and carbonates. The characteristic quartz bands are not affected by the heat treatment.

3.1.2. Kaolinite

The kaolinite analyzed comes from the Oulmès region near Rabat and has a high fraction of particles smaller than 5 μm as shown in Table 2.

Fig. 10 shows the morphology of the studied kaolinite. We note the existence of layered grains in its structure.

The chemical composition and surface analysis of kaolinite are presented in Table 3 and Fig. 11. From these analyses, it appears that kaolinite consists mainly of silica and alumina. The alkaline and alkaline earth element contents are low.

Fig. 12 shows the diffractograms of natural kaolinite and calcined kaolinite at different temperatures. The diffractogram of raw kaolinite reveals, on the one hand, a strong presence of silica, mainly in the form of quartz, and on the other hand that kaolinite and illite are the main phyllite phases

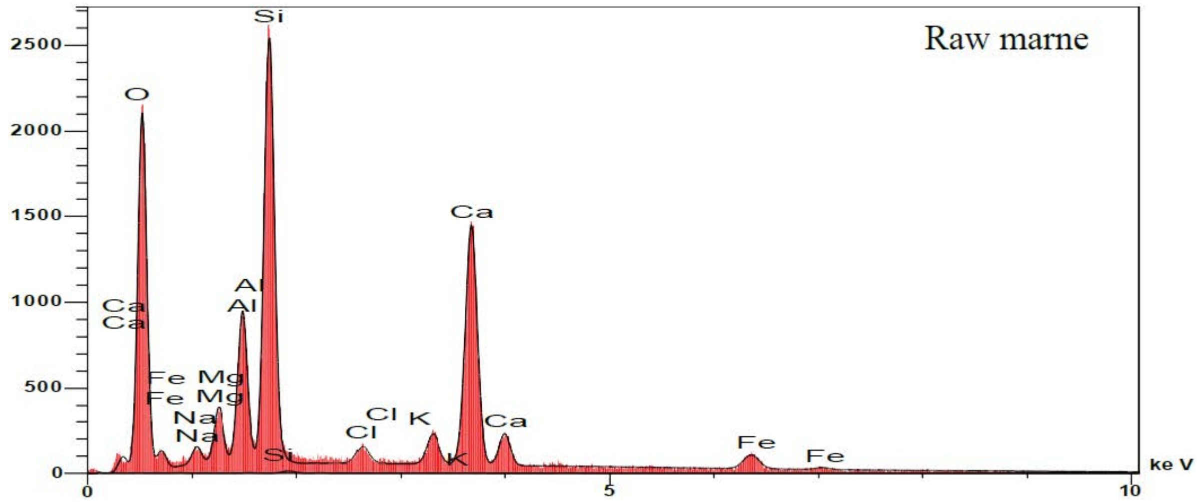

Fig. 3. EDS of the raw yellow marl.

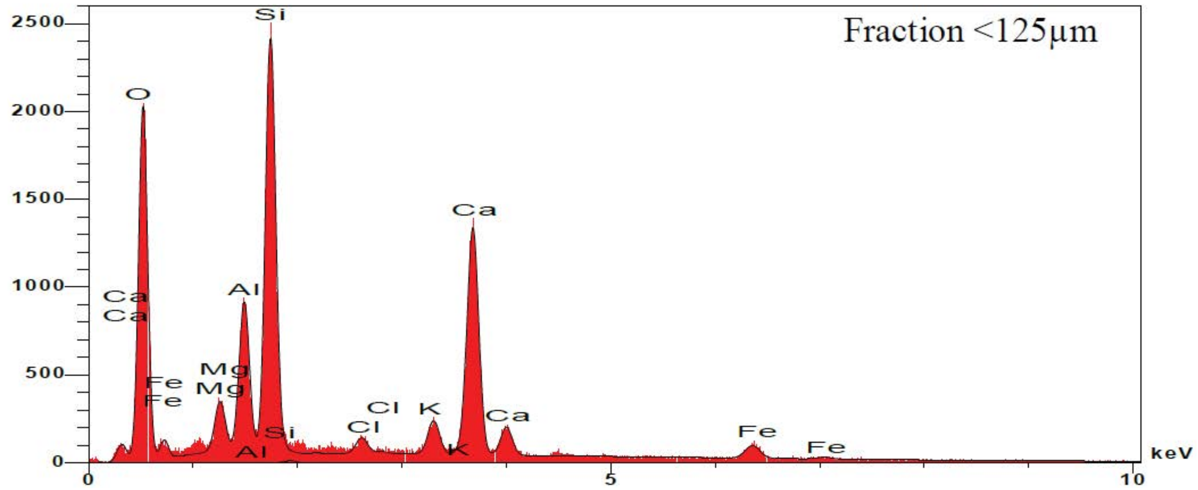

Fig. 4. EDS of the powder yellow marl sieved to <125 μm.

Table 1
Weight and atomic percentages of chemical elements in yellow marl

Element	Raw yellow marl		Yellow marl (≤125 μm)	
	Weight %	Atomic %	Weight %	Atomic %
O	46.37	63.79	47.39	64.74
Na	1.11	1.06	–	–
Mg	2.63	2.38	2.75	2.47
Al	6.40	5.22	6.96	5.64
Si	17.70	13.87	18.00	14.01
Cl	1.10	0.68	1.01	0.62
K	2.24	1.26	2.38	1.33
Ca	18.61	10.22	18.00	9.81
Fe	3.84	1.51	3.52	1.38

present in the sample. Heat treatment at 600°C results in the disappearance of all reflections characteristic of kaolinite, this treatment seems to have no effect on illite. This phenomenon has already been observed by several authors and is the result of the dehydroxylation of kaolinite to meta-kaolinite which presents a poorly organized structure. Heat treatment at 1,250°C results in the appearance of new lines associated with the formation of mullite crystals and the disappearance of the characteristic lines of illite.

The two DTA and TGA curves of kaolinite are shown in Fig. 13. They were carried out in the air with a temperature rise of 5°C/min to 1,250°C.

The TGA of kaolinite shows that during the heating, there are two weight losses corresponding to the total loss of the initial mass of the sample of 6.9%. The first loss starts around 35°C and ends around 200°C, it is mainly due to the departure of physisorbed water. The second loss starts at about 400°C and ends at about 780°C, it corresponds to the dehydroxylation phenomenon which marks the destruction of the kaolinite structure. On the DTA

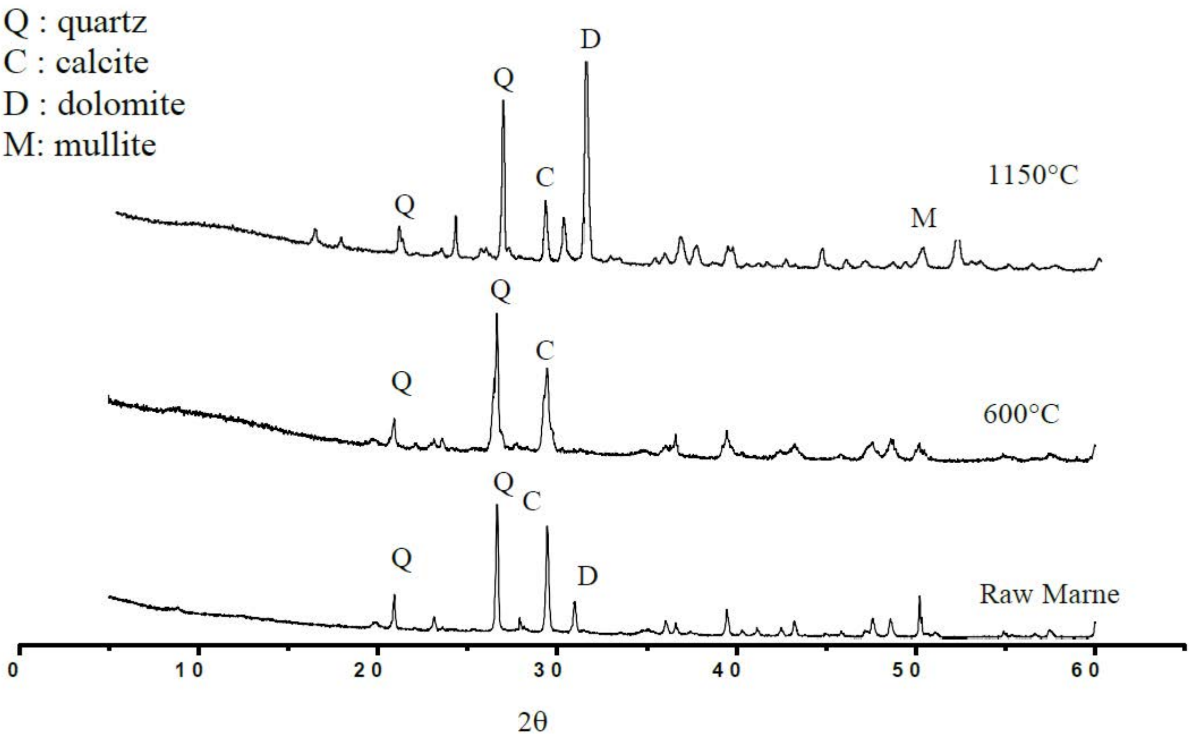

Fig. 5. X-ray diffraction patterns of yellow marl treated at various temperatures.

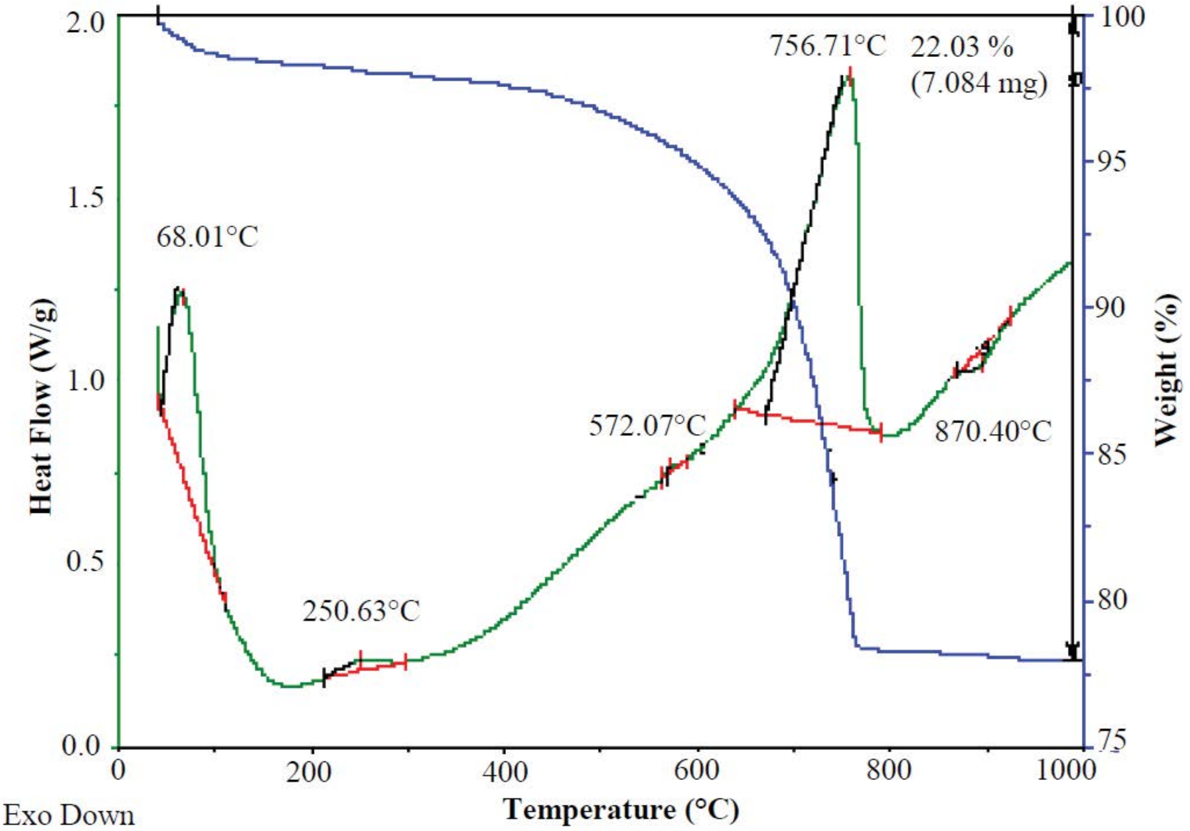

Fig. 6. TGA/DTA for yellow marl sieved to <125 μm.

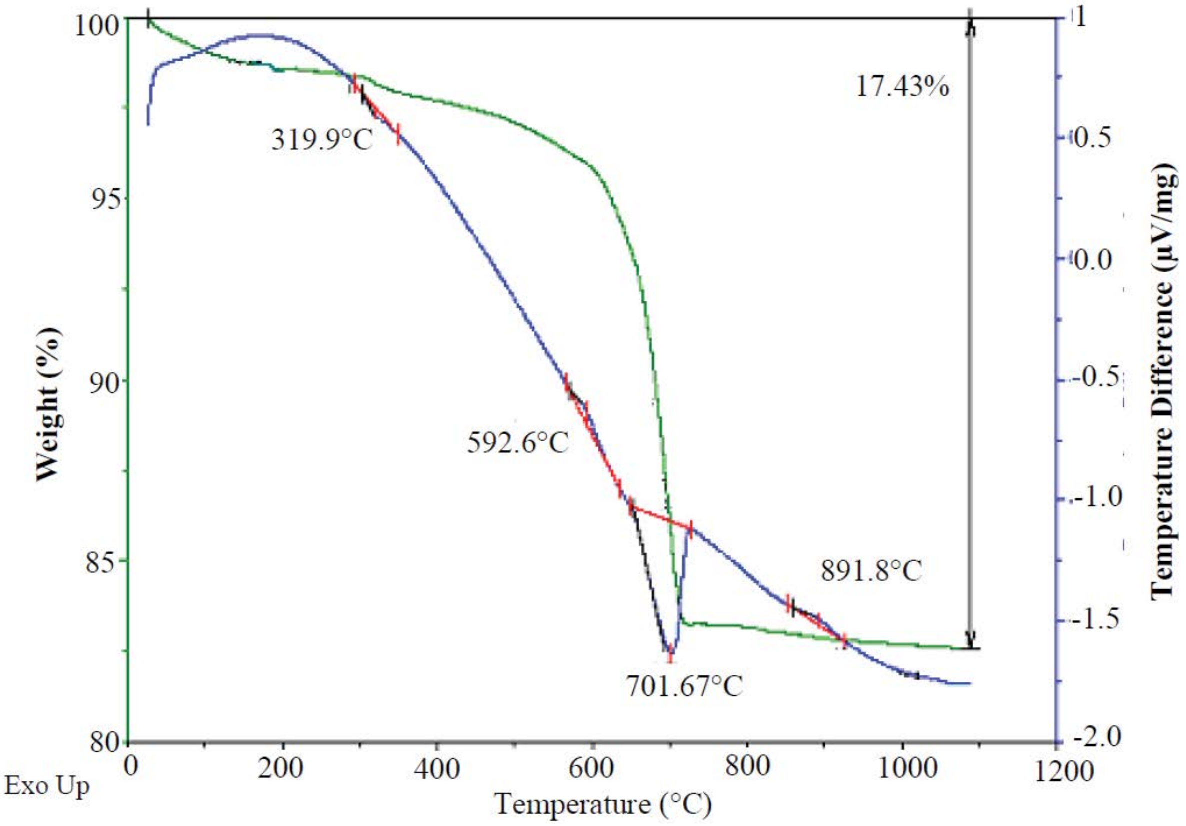

Fig. 7. TGA/DTA for yellow marl treated at 600°C.

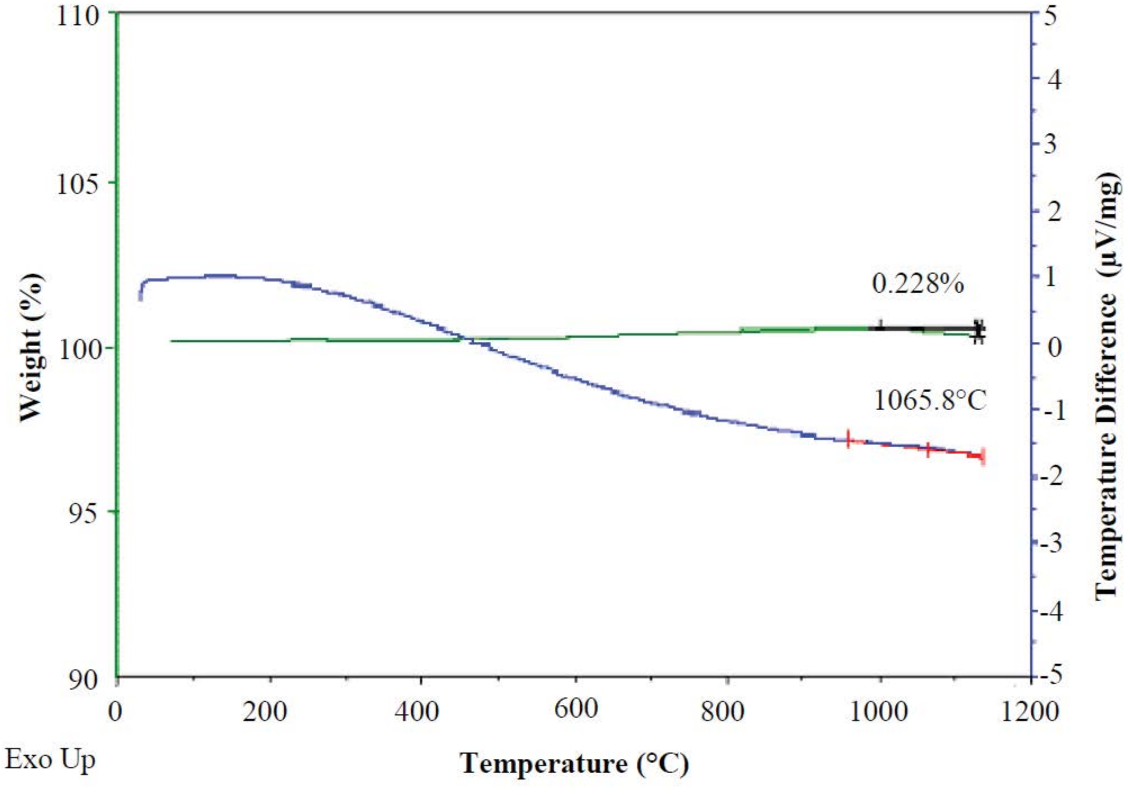

Fig. 8. TGA/DTA for yellow marl treated at 1,150°C.

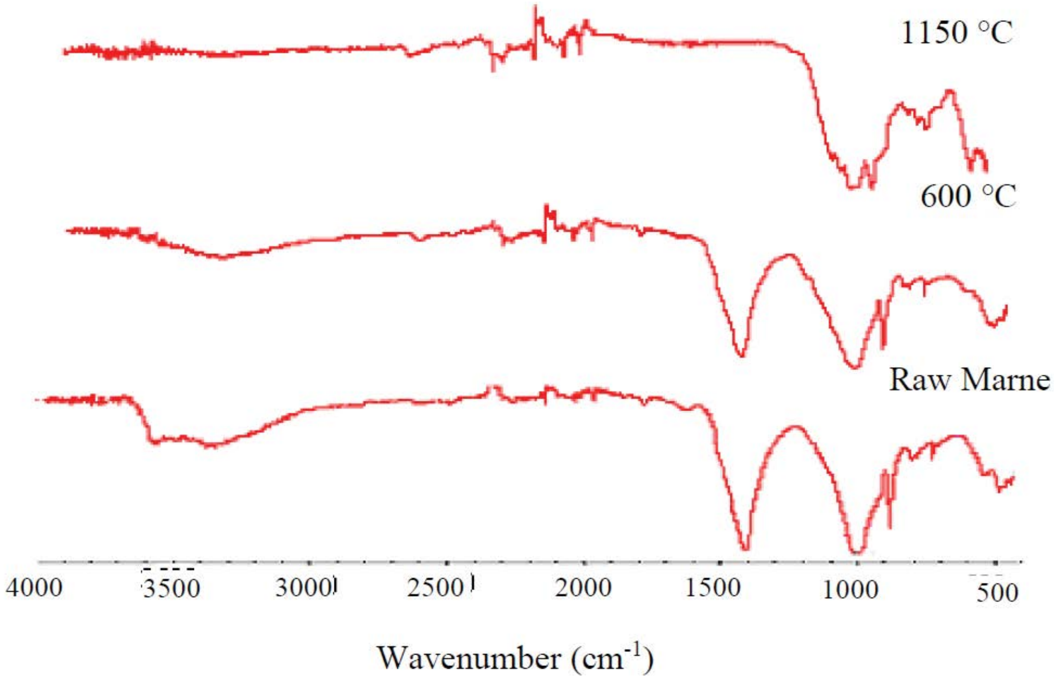

Fig. 9. Fourier transform infrared spectra of yellow marl treated at various temperatures.

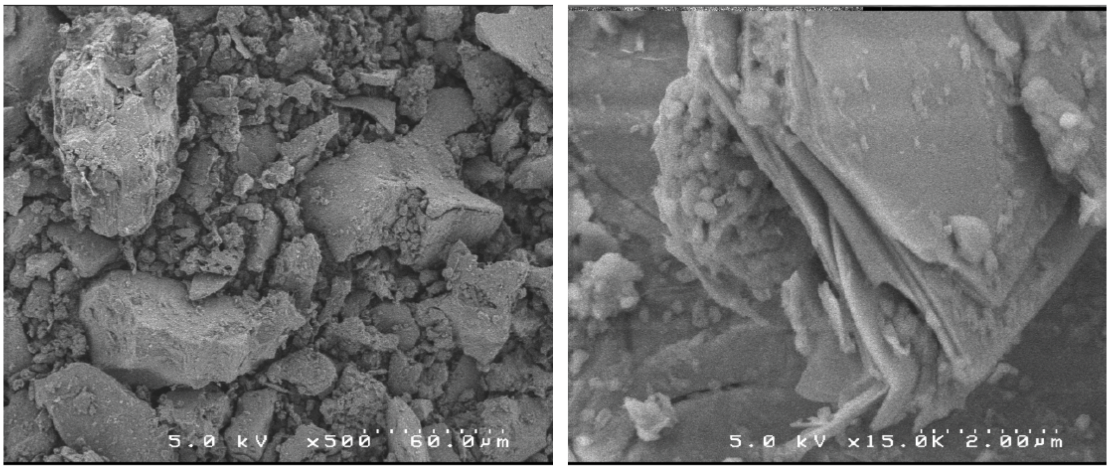

Fig. 10. SEM of the powder kaolinite.

Table 2
Kaolinite particle size distribution

Particle diameter (µm)	Ratio (%)
[10,36]	4.342
[5,10]	12.618
<5	83.040

curve, three endothermic peaks are observed at <100°C, 520°C and 570°C, which corresponds respectively to the departure of physisorbed water, to the dehydroxylation of kaolinite and to the transformation of a-quartz to b-quartz. To this is added the presence of an exothermic peak at

Table 3
Chemical composition of kaolinite

Oxide	Weight %
SiO_2	80.00
Al_2O_3	12.09
Fe_2O_3	1.00
Na_2O	0.50
K_2O	3.73
CaO	1.21
MgO	0.06
TiO_2	1.21
SO_2	<0.2

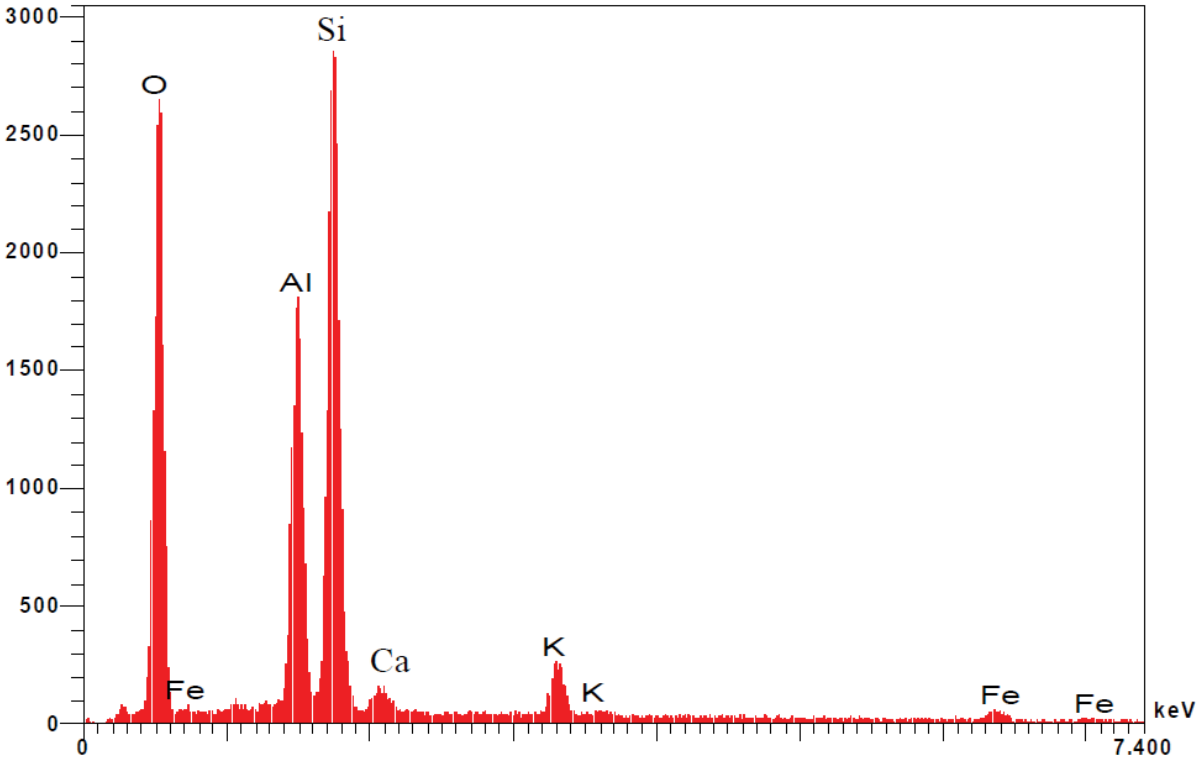

Fig. 11. EDS of the powder kaolinite.

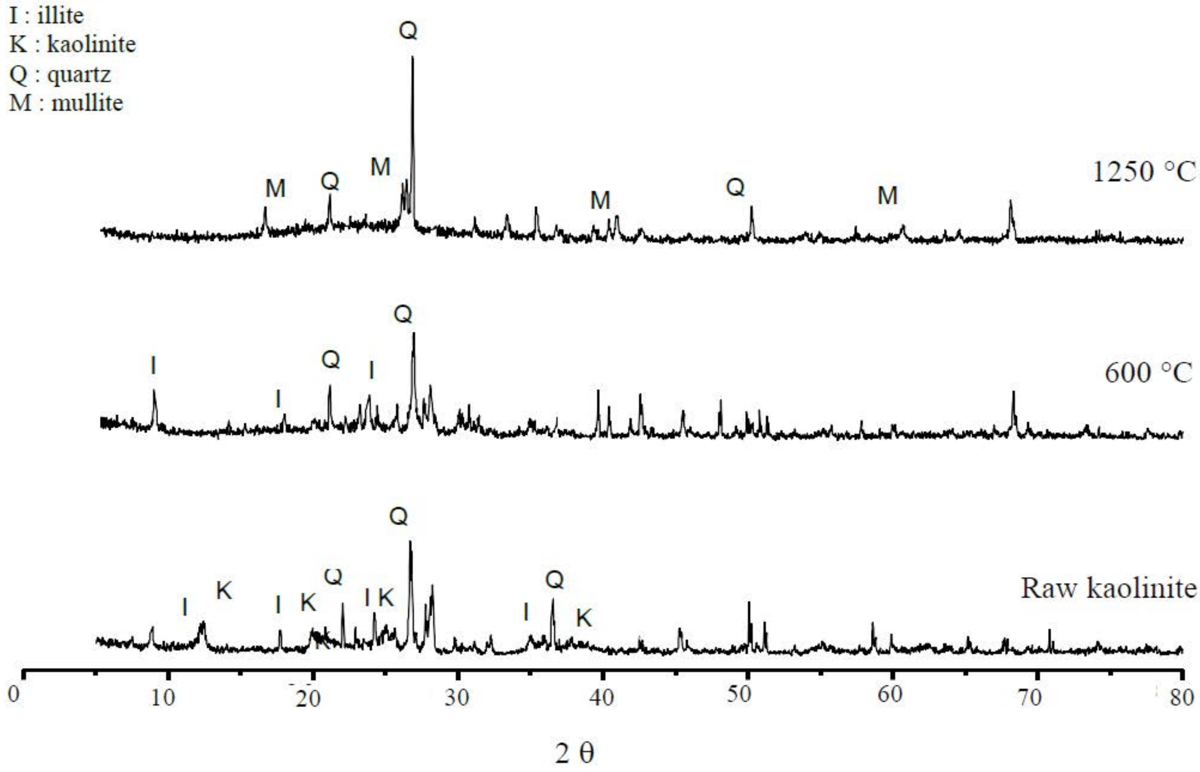

Fig. 12. X-ray diffraction patterns of kaolinite treated at various temperatures.

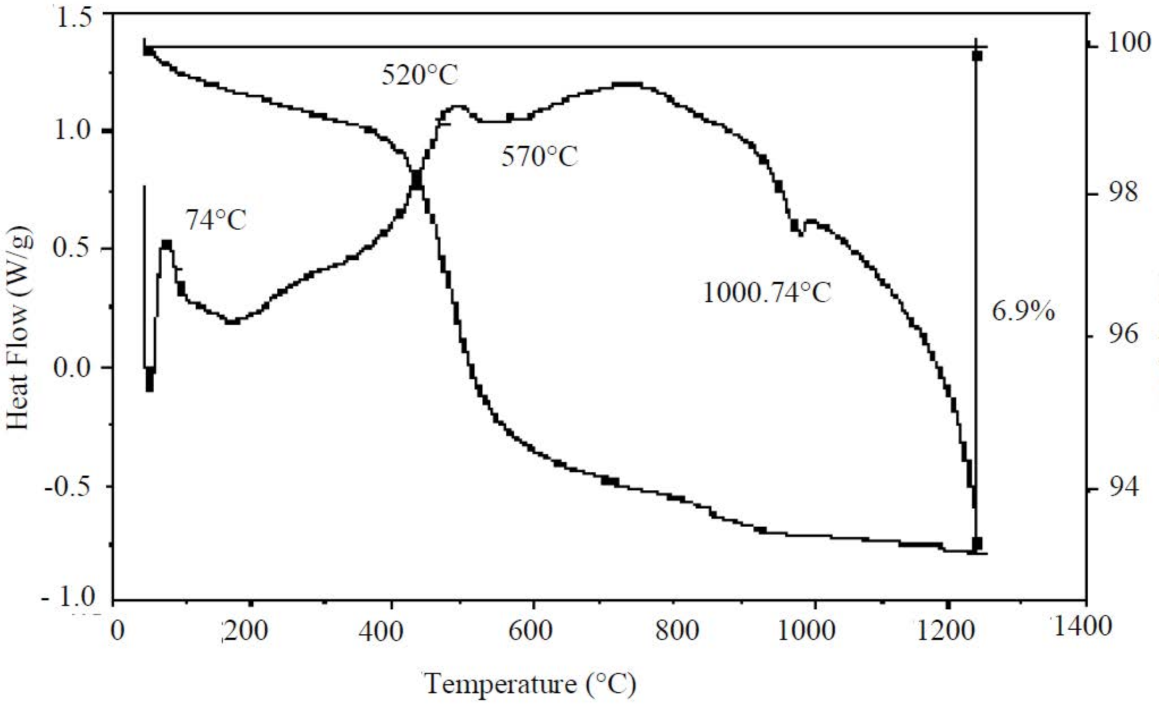

Fig. 13. DTA/TGA of the powder kaolinite.

around 1,000°C which corresponds to the mullite phase crystallization phenomenon.

3.2. Adsorption study

Generally speaking, adsorption is defined as a process resulting from a net accumulation of a substance at the interface between two contiguous phases [20–24]. It is therefore a surface phenomenon, and the ions and molecules adsorbed do not in any way become part of the structure of the solid on which they are adsorbed. The term adsorption does not specify the nature of the reaction between the adsorbed solute and the solid phase.

Two modes of adsorption are generally proposed to describe the retention of molecules on the surface of the adsorbent namely, chemical adsorption and physical adsorption. Chemical adsorption (specific or chemisorption) corresponds to the establishment of chemical bonds between the surface of the adsorbent and the adsorbed molecule, and therefore depends on the surface chemical properties (functional groups) of the adsorbent. It is an often irreversible fixation on specific sites. Physical adsorption (non-specific or physisorption) involves Van Der Waals type forces between the surface of the adsorbent and the molecules physisorbed on it. It is a reversible process (dynamic equilibrium of adsorption and desorption) that preserves the chemical identity of the adsorbed molecule.

Despite the importance of the physico-chemical studies undertaken on the retention of organic matter, several factors influencing the efficiency of an adsorbent remain unknown. Among the parameters that intervene during adsorption. We can mention, the physico-chemical properties of the solute, the properties of the adsorbent, the physico-chemical properties of the aqueous phase and the presence of several solutes.

The effect of varying the concentration of methylene blue on the removal efficiency for the two clays is shown in Fig. 14.

For yellow marl, there is the complete removal of MB dye for concentrations between 100 and 550 ppm, beyond which it starts to decrease. For kaolinite, the maximum removal efficiency is less important than that of yellow marl, it is between 100 and 200 ppm and starts to decrease from 300 ppm. This can be explained by the saturation of the number of available sites at high dye concentrations [25–29].

The equilibrium between the adsorbent in the liquid phase and the adsorbent fixed on the solid is reached with a rapidity that depends not only on the diffusion rate of the components in the adsorbent and in the fluid but also on the adsorbent–adsorbate interface. The study of the adsorption of a compound on an adsorbent makes it is possible to examine the influence of the contact time on its retention.

The study of decomposition kinetics is a very important step in determining the time required to reach equilibrium. It was carried out in order to determine the stationary quantities of methylene blue from the contact time to equilibrium. The methylene blue concentrations, the masses of the adsorbent and the flasks are all identical. The results are shown in Fig. 15. The adsorption of methylene blue was found to be faster for yellow marl, which is probably related to the physico-chemical properties of this clay and more particularly to the nature of the sites, the specific surface and the porosity of the support. Equilibrium is reached after 60 min for yellow marl and 150 min for kaolinite. Usually, an adsorption mechanism comprises the following general steps: migration of the dye from the solution to the surface

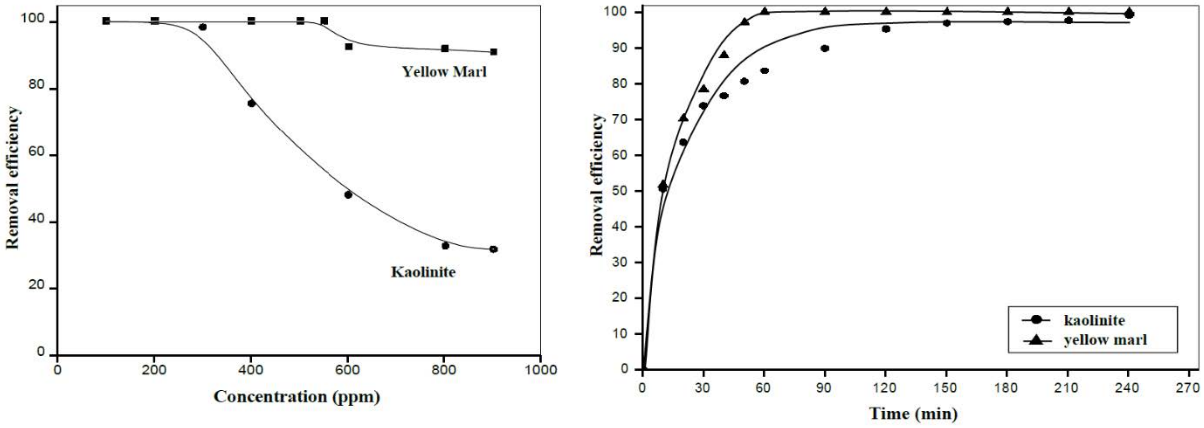

Fig. 14. Adsorption of methylene blue on pre-treated Moroccan natural clays.

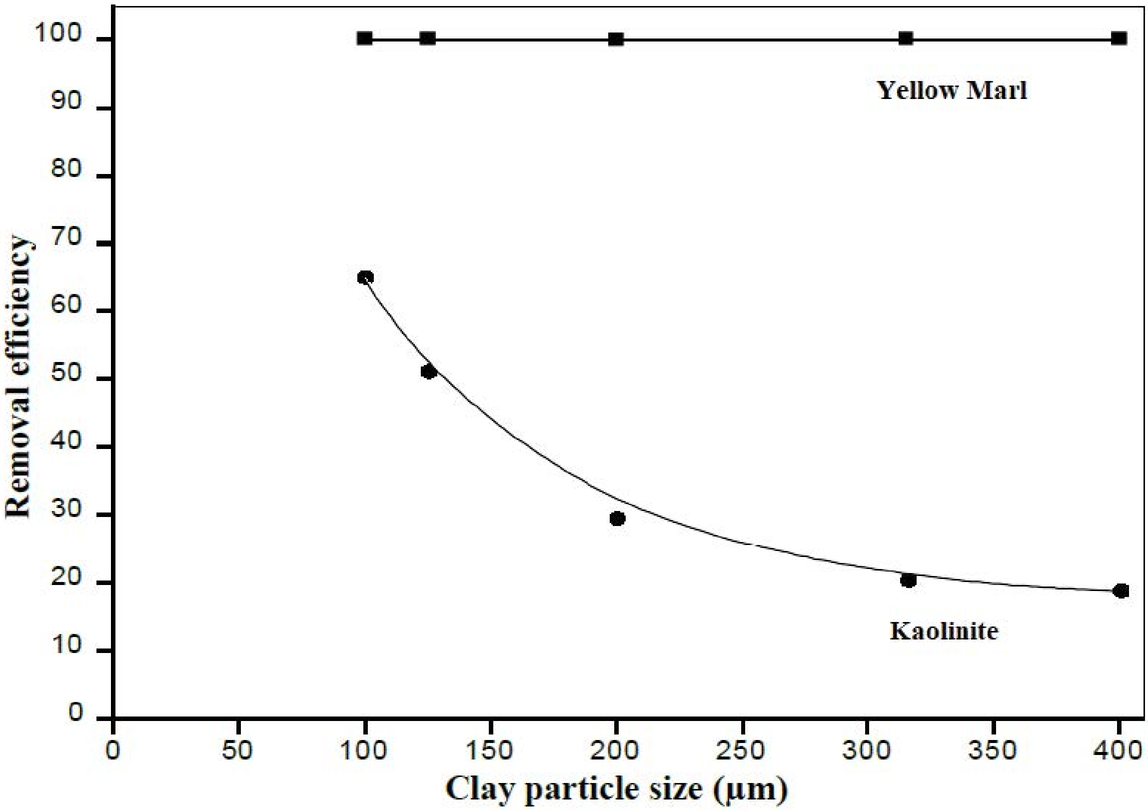

Fig. 15. Effect of clay particle size on the removal efficiency of MB dye.

of the adsorbent, diffusion of the dye through the diffusion layer, adsorption of the dye on the active sites of the clay and intraparticle diffusion of the dye to the internal clay pores.

The effect of clay particle size on the removal efficiency of MB dye is shown in Fig. 15. The particle size of the yellow marl has no effect on the removal efficiency of methylene blue, a total removal is seen for all the particle sizes studied, on the other hand for kaolinite the removal efficiency decreases when the particle size increases, this is due to the increase in the specific area of the clay when the particle size becomes finer [30]. This is why we chose to work with a granulometry lower than 0.05 mm for both clays in order to have a better dye removal. The pH effect on the removal efficiency of methylene blue by yellow marl and kaolinite are reported in Fig. 16.

Fig. 16 shows that the pH has no influence on the removal efficiency of methylene blue by the yellow marl, whatever the concentration of the solution.

Fig. 16 also shows that the removal efficiency of methylene blue by kaolinite is better in basic media for concentrations ranging from 200 to 400 ppm. The decrease in the removal

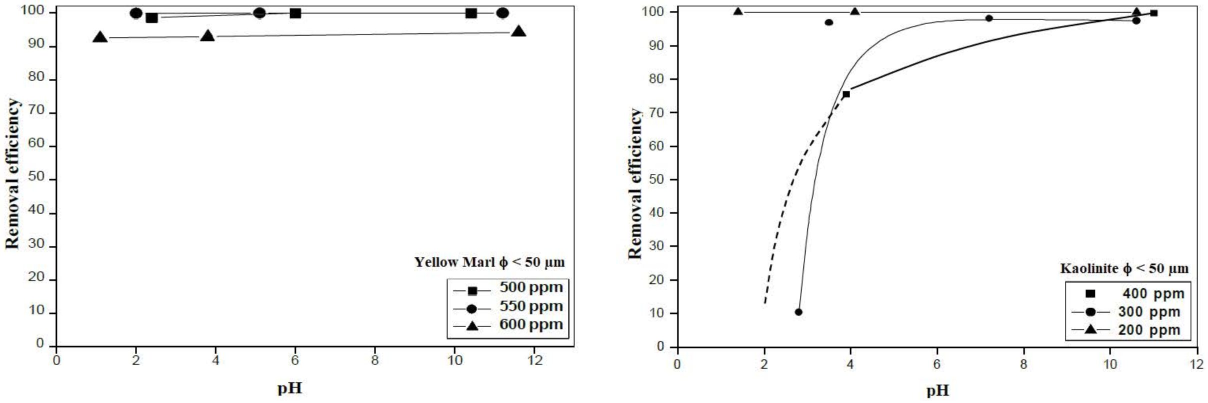

Fig. 16. Effect of pH on adsorption of MB by pre-treated Moroccan natural clays.

efficiency in the acidic medium (pH < 3) can be explained by the competition between the protons and the molecules of the cationic dye with regard to the retention sites.

4. Conclusion

The study of the absorption of methylene blue on two clays (yellow marl and kaolinite) was carried out in static mode at 25°C. This adsorption is dependent on the type of adsorbent, the initial dye concentrations, the granulometry of the adsorbent and the pH of the environment. Yellow marl showed a higher dye-binding capacity than kaolinite at the different concentrations and particle sizes and pH levels studied. Kaolinite adsorbed better towards basic pH. The adsorbed quantities at equilibrium reached 27.5 mg g^{-1} for yellow marl and 16 mg g^{-1} for kaolinite. The difference in adsorption capacity between both clays studied is due to the percentage of the clay phase in each and to its composition. These results encourage us to use yellow marl as clay support in the preparation of a ceramic membrane for future application in the ultrafiltration of industrial wastewater.

References

[1] M. Kastali, L. Mouhir, M. Assou, A. Anouzla, Y. Abrouki, Diagnosis of leachate from a closed landfill, impact on the soil, and treatment by coagulation flocculation with alginate and ferric chloride, Desal. Water Treat., 206 (2020) 307–314.

[2] M. Kastali, L. Mouhir, M. Chatoui, S. Souabi, A. Anouzla, Removal of turbidity and sludge production from industrial process wastewater treatment by a rejection of steel rich in FeCl$_3$ (SIWW), Biointerface Res. Appl. Chem., 11 (2021) 13359–13376.

[3] M. Iqbal, *Vicia faba* bioassay for environmental toxicity monitoring: a review, Chemosphere, 144 (2016) 785–802.

[4] M. Abbas, M. Adil, S. Ehtisham-ul-Haque, B. Munir, M. Yameen, A. Ghaffar, G.A. Shar, M.A. Tahir, M. Iqbal, *Vibrio fischeri* bioluminescence inhibition assay for ecotoxicity assessment: a review, Sci. Total Environ., 626 (2018) 1295–1309.

[5] M. Iqbal, M. Abbas, J. Nisar, A. Nazir, Bioassays based on higher plants as excellent dosimeters for ecotoxicity monitoring: a review, Chem. Int., 5 (2019) 1–80, doi: 10.5281/zenodo.1475399.

[6] J. Mabrouki, A. Moufti, I. Bencheikh, K. Azoulay, Y. El Hamdouni, S. El Hajjaji, Optimization of the Coagulant Flocculation Process for Treatment of Leachate of the Controlled Discharge of the City Mohammedia (Morocco), International Conference on Advanced Intelligent Systems for Sustainable Development, 2019, pp. 200–212.

[7] A. Anouzla, Y. Abrouki, S. Souabi, M. Safi, H. Rhbal, Colour and COD removal of disperse dye solution by a novel coagulant: application of statistical design for the optimization and regression analysis, J. Hazard. Mater., 166 (2009) 1302–1306.

[8] J. Mabrouki, I. Bencheikh, K. Azoulay, M. Es-Soufy, S. El Hajjaji, Smart Monitoring System for the Long-Term Control of Aerobic Leachate Treatment: Dumping Case Mohammedia (Morocco), International Conference on Big Data and Networks Technologies, 2019, pp. 220–230.

[9] K. Azoulay, I. Bencheikh, A. Moufti, A. Dahchour, J. Mabrouki, S. El Hajjaji, Comparative study between static and dynamic adsorption efficiency of dyes by the mixture of palm waste using the central composite design, Chem. Data Collect., 27 (2020) 100385, doi: 10.1016/j.cdc.2020.100385.

[10] N.A. Lutpi, T.H. Yin, W.Y. Shian, A.N. Kamarudzaman, Removal of Methylene Blue Using Pineapple Peel Powder as Adsorbent, Proceedings of the 3rd CUTSE International Conference Miri, Sarawak, Malaysia, 2011, pp. 352–356.

[11] J. Mabrouki, G. Fattah, N. Al-Jadabi, Y. Abrouki, D. Dhiba, M. Azrour, S. El Hajjaji, Study, simulation and modulation of solar thermal domestic hot water production systems, Model. Earth Syst. Environ., (2021), doi: 10.1007/s40808-021-01200-w.

[12] I. Bencheikh, K. Azoulay, J. Mabrouki, S. El Hajjaji, A. Moufti, N. Labjar, The use and the performance of chemically treated artichoke leaves for textile industrial effluents treatment, Chem. Data Collect., 31 (2021) 100597, doi: 10.1016/j.cdc.2020.100597.

[13] K. Azoulay, I. Bencheikh, J. Mabrouki, N. Samghouli, A. Moufti, A. Dahchour, S. El Hajjaji, Adsorption mechanisms of azo dyes binary mixture onto different raw palm wastes, Int. J. Environ. Anal. Chem., 101 (2021) 1–20.

[14] A.A. Inyinbor, F.A. Adekola, G.A. Olatunji, Kinetics, isotherms and thermodynamic modeling of liquid phase adsorption of Rhodamine B dye onto *Raphia hookerie* fruit epicarp, Water Resour. Ind., 15 (2016) 14–27.

[15] M.T. Yagub, T.K. Sen, H.M. Ang, Equilibrium, kinetics, and thermodynamics of methylene blue adsorption by pine tree leaves, Water Air Soil Pollut., 223 (2012) 5267–5282.

[16] J. Mabrouki, M. Benbouzid, D. Dhiba, S. El Hajjaji, Simulation of wastewater treatment processes with Bioreactor Membrane Reactor (MBR) treatment versus conventional the adsorbent layer-based filtration system (LAFS), Int. J. Environ. Anal. Chem., (2020) 1–11, doi: 10.1080/03067319.2020.1828394.

[17] S.N. Jain, S.R. Tamboli, D.S. Sutar, S.R. Jadhav, J.V. Marathe, A.A. Shaikh, A.A. Prajapati, Batch and continuous studies for adsorption of anionic dye onto waste tea residue: kinetic, equilibrium, breakthrough and reusability studies, J. Cleaner Prod., 252 (2020) 1–15, doi: 10.1016/j.jclepro.2019.119778.

[18] A. Kriaa, N. Hamdi, E. Srasra, Adsorption studies of methylene blue dye on Tunisian activated lignin, Russ. J. Phys. Chem. A, 85 (2011) 279–287.

[19] P.S. Kumar, S. Ramalingam, K. Sathishkumar, Removal of methylene blue dye from aqueous solution by activated carbon

prepared from cashew nut shell as a new low-cost adsorbent, Korean J. Chem. Eng., 28 (2011) 149–155.

[20] P.M.K. Reddy, P. Verma, C. Subrahmanyam, Bio-waste derived adsorbent material for methylene blue adsorption, J. Taiwan Inst. Chem. Eng., 58 (2015) 500–508.

[21] D. Pathania, S. Sharma, P. Singh, Removal of methylene blue by adsorption onto activated carbon developed from *Ficus carica* bast, Arabian J. Chem., 10 (2017) S1445–S1451.

[22] J. Goscianska, N.A. Fathy, R.M.M. Aboelenin, Adsorption of solophenyl red 3BL polyazo dye onto amine-functionalized mesoporous carbons, J. Colloid Interface Sci., 505 (2017) 593–604.

[23] Y. Miyah, A. Lahrichi, M. Idrissi, A. Khalil, F. Zerrouq, Adsorption of methylene blue dye from aqueous solutions onto walnut shells powder: equilibrium and kinetic studies, Surf. Interfaces, 11 (2018) 74–81.

[24] M.Z. Bin Mukhlish, M.R. Khan, M.C. Bhoumick, S. Paul, Papaya (*Carica papaya* L.) leaf powder: novel adsorbent for removal of methylene blue from aqueous solution, Water Air Soil Pollut., 223 (2012) 4949–4958.

[25] R. El Haouti, H. Ouachtak, A. El Guerdaoui, A. Amedlous, E. Amaterz, R. Haounati, A.A. Addi, F. Akbal, N. El Alem, M.L. Taha, Cationic dyes adsorption by Na-montmorillonite nano clay: experimental study combined with a theoretical investigation using DFT-based descriptors and molecular dynamics simulations, J. Mol. Liq., 290 (2019) 1–15, doi: 10.1016/j.molliq.2019.111139.

[26] A.B. Albadarin, M.N. Collins, M. Naushad, S. Shirazian, G. Walker, C. Mangwandi, Activated lignin-chitosan extruded blends for efficient adsorption of methylene blue, Chem. Eng. J., 307 (2017) 264–272.

[27] M. Pirsaheb, Z. Rezai, A.M. Mansouri, A. Rastegar, A. Alahabadi, A.R. Sani, K. Sharafi, Preparation of the activated carbon from India shrub wood and their application for methylene blue removal: modeling and optimization, Desal. Water Treat., 57 (2016) 5888–5902.

[28] B. Sadhukhan, N.K. Mondal, S. Chattoraj, Optimisation using central composite design (CCD) and the desirability function for sorption of methylene blue from aqueous solution onto Lemna major, Karbala Int. J. Mod. Sci., 2 (2016) 145–155.

[29] H. Ouachtak, R. El Haouti, A. El Guerdaoui, R. Haounati, E. Amaterz, A.A. Addi, F. Akbal, M.L. Taha, Experimental and molecular dynamics simulation study on the adsorption of Rhodamine B dye on magnetic montmorillonite composite γ-Fe_2O_3@Mt, J. Mol. Liq., 309 (2020) 1–17, doi: 10.1016/j.molliq.2020.113142.

[30] F. Largo, R. Haounati, S. Akhouairi, H. Ouachtak, R. El Haouti, A. El Guerdaoui, N. Hafid, D.M.F. Santos, F. Akbal, A. Kuleyin, A. Jada, A.A. Addi, Adsorptive removal of both cationic and anionic dyes by using sepiolite clay mineral as adsorbent: experimental and molecular dynamic simulation studies, J. Mol. Liq., 318 (2020) 1–14, doi: 10.1016/j.molliq.2020.114247.